

# Analysis of time-dependent change of *Escherichia coli* $F_1$ -ATPase activity and its relationship with apparent negative cooperativity

Yasuyuki Kato, Takeshi Sasayama, Eiro Muneyuki<sup>\*</sup>, Masasuke Yoshida

Research Laboratory of Resources Utilization, R-1, Tokyo Institute of Technology, 4259 Nagatsuta, Midori-ku, Yokohama, Kanagawa 226, Japan

Received 20 March 1995; accepted 15 May 1995

## Abstract

Except for the case of gradual activation of  $EF_1$  ( $F_1$ -ATPase from *Escherichia coli*) caused by the dissociation of the  $\epsilon$  subunit [Laget, P.P. and Smith, J.B. (1979) Arch. Biochem. Biophys. 197, 83–89],  $EF_1$  has long been thought not to show a time-dependent change in activity [Senior, A.E. et al. (1992) Arch. Biochem. Biophys. 297, 340–344]. Here, we report the time-dependent inactivation and activation of  $EF_1$ , which are apparently similar to those of mitochondrial  $F_1$ -ATPases [Vasilyeva, E.A. et al. (1982) Biochem. J. 202, 15–23]. Analysis of these changes as a function of ATP concentrations in relation to negative cooperativity revealed that the initial inactivation phase was attributable to the decrease in the  $V_{\max}$  associated with the low  $K_m$  (around 10  $\mu$ M), and the following activation, probably due to the dissociation of the  $\epsilon$  subunit, corresponded to the increase in the  $V_{\max}$  associated with the high  $K_m$  (in the order of 100  $\mu$ M). Thus, the time-dependent change in  $EF_1$  activity is closely related to the apparent negative cooperativity (multiple  $K_m$  values) of ATP hydrolysis.

**Keywords:** Cooperativity; Kinetics; ATPase,  $F_1$ -

## 1. Introduction

The  $F_0F_1$ -ATP synthase of *Escherichia coli* plays an important role in oxidative phosphorylation by coupling transmembrane proton flow and ATP synthesis [1,2].  $F_1$  is the water-soluble membrane peripheral part of  $F_0F_1$  and has catalytic sites for ATP synthesis and hydrolysis. Its subunit composition is  $\alpha_3\beta_3\gamma\delta\epsilon$ . The  $F_0$  portion is a membrane-embedded proton channel.  $F_1$ , when isolated from the membrane, catalyzes net ATP hydrolysis and its mechanism has been extensively investigated on the assumption that the hydrolysis is the reverse reaction of synthesis [2]. One of the most prominent characteristics of ATP hydrolysis catalyzed by  $F_1$  is the apparent negative cooperativity [3,4] which is also observed for the mem-

brane-bound enzyme [5,6]. In addition, the  $F_1$ -ATPase from bovine heart mitochondria ( $MF_1$ ) shows an initial inactivation [7–10] and activation during the ATP hydrolysis reaction [11]. These characteristics are thought to reflect interactions between multiple catalytic sites or non-catalytic sites and catalytic sites [11,12]. However, such an inactivation or activation has not been reported in the case of the  $F_1$  from *E. coli* ( $EF_1$ ), except for the case of the activation caused by the dissociation of the  $\epsilon$  subunit from the enzyme molecule [13–15].

In the present study, we demonstrate that  $EF_1$  also exhibits the time-dependent initial inactivation followed by slow activation like  $MF_1$ . We analyzed the time-dependent change in ATPase activity in relation to the apparent negative cooperativity (expressed by multiple  $K_m$  values) and found that they are closely related to each other. The initial inactivation corresponded to the decrease in the  $V_{\max}$  associated with the low  $K_m$  (around 10  $\mu$ M), and the following activation, which is most likely caused by the dissociation of the  $\epsilon$  subunit, corresponded to the increase in the  $V_{\max}$  associated with the high  $K_m$  (in the order of 100  $\mu$ M).

Abbreviations:  $EF_1$ ,  $F_1$ -ATPase from *Escherichia coli*;  $MF_1$ ,  $F_1$ -ATPase from mitochondria; HPLC, high-performance liquid chromatography; DTT, dithiothreitol; nd- $EF_1$ ,  $EF_1$  depleted of nucleotides.

<sup>\*</sup> Corresponding author. Fax: +81 45 9245277, e-mail address: emuneyuk@res.titech.ac.jp.

## 2. Materials and methods

### 2.1. Preparation of native $EF_1$ and nd- $EF_1$

Native  $EF_1$  was prepared according to Wise [16] with some modifications as follows. After solubilization, the crude  $EF_1$  fraction was directly applied on a DEAE-Toyopearl ion-exchange column (Tosoh, Japan). Peak protein fractions were collected and precipitated with 65% saturated ammonium sulfate. The enzyme was then further purified with a G3000SW gel-filtration HPLC column (Tosoh, Japan) equilibrated and eluted (flow rate: 1 ml/min.) with 50 mM Tris-HCl (pH 7.4), 10% (v/v) methanol, 40 mM 6-aminohexanoic acid, 2 mM EDTA, 1 mM ATP, 1 mM DTT and 150 mM  $Na_2SO_4$ . Peak protein fractions were collected and precipitated with 65% saturated ammonium sulfate. Purified  $EF_1$  (precipitant) was dissolved in the storage buffer consisting of 50 mM Tris- $H_2SO_4$  (pH 7.5), 2 mM EDTA, 1 mM DTT, 40 mM 6-aminohexanoic acid, 10% (v/v) glycerol and 1 mM ATP, and stored at  $-20^\circ C$ . The specific activity at  $37^\circ C$  and 5 mM of ATP was about 80 U/mg.  $EF_1$  depleted of nucleotides (nd- $EF_1$ ) was prepared according to Senior et al. [17]. The nd- $EF_1$  was stored at room temperature in 100 mM Tris- $H_2SO_4$  (pH 8.0) containing 4 mM EDTA and 50% (v/v) glycerol. The specific activity was about 75 U/mg at  $37^\circ C$ . The amounts of bound nucleotides were analyzed by HPLC [18]. Native  $EF_1$  used in this study contained about 1.4 mol of ADP/mol of enzyme and 0.6 mol of ATP/mol of enzyme. nd- $EF_1$  contained about 0.1 mol of ADP/mol of enzyme and essentially no ATP. Protein concentration was measured by the method of Bradford [19].

### 2.2. Measurement of ATPase activity

The ATPase activity of  $EF_1$  was measured spectrophotometrically using an ATP regenerating system [20] at  $25^\circ C$  with the spectrophotometer UV-2200 (Shimadzu, Japan). Before measurement of ATPase activity,  $EF_1$  was passed through a 1 ml of Sephadex G-50 fine centrifuge column [21] twice to remove ATP in the storage buffer. In the case of nd- $EF_1$ , there is no ATP in the sample buffer, and this step was omitted. The enzyme was then diluted to about 0.2  $\mu M$  in a buffer containing 50 mM Tris- $H_2SO_4$  (pH 8.0), 2 mM EDTA, 1 mM DTT, 40 mM 6-aminohexanoic acid and 10% (v/v) glycerol to avoid irreversible inactivation during the experiment. The basic assay medium consisted of 50 mM Tris- $H_2SO_4$  (pH 8.0), 10 mM KCl, 2.5 mM phosphoenolpyruvate, 0.15–0.3 mM NADH, 50  $\mu g/ml$  pyruvate kinase, 50  $\mu g/ml$  lactate dehydrogenase (both enzymes were obtained from Boehringer in 50% glycerol) and 2 mM  $MgSO_4$ . In a preliminary experiment, we tested different amounts of coupling enzymes in the assay mixture and confirmed that the above condition is sufficient to follow the ATPase activity within the time

scale employed here. When a buffer system containing chloride instead of sulfate was employed, qualitatively the same results as shown in Results were obtained. When the ATPase reaction was started by the addition of  $EF_1$  to the basic assay medium ( $F_1$ -started), various concentrations of Mg-ATP (1–5000  $\mu M$ ) were added to the basic assay medium before the  $EF_1$  addition. The reaction was then initiated by the addition of  $EF_1$  solution to a final concentration of about 3 nM. The time-course of the data was collected every 0.5 s for 630 s and stored in an on-line computer. When the ATPase reaction was started by the addition of ATP (ATP-started),  $EF_1$  was added to the assay medium at a concentration of about 3 nM and previously incubated at  $37^\circ C$  for at least 15 min to complete the activation. (At  $25^\circ C$ , the activation took about 1 h in the absence of adenine nucleotides (data not shown).) The assay medium was then cooled to  $25^\circ C$  and the reaction was initiated by the addition of stock ATP-Mg solution. The stock ATP-Mg solution was prepared by mixing the basic assay medium containing the ATP regenerating system with concentrated ATP-Mg solution to remove the contaminated ADP. Final ATP concentrations were varied from 1  $\mu M$  to 1500  $\mu M$ . One unit of enzyme activity was defined as that producing 1  $\mu mol$  of ADP per minute.

## 3. Results

### 3.1. ATP hydrolysis initiated by the addition of $EF_1$

Typical time-courses of ATP hydrolysis are shown in Fig. 1. The reaction was initiated by the addition of  $F_1$  ( $F_1$ -started). Fig. 1A shows the traces of the absorbance change at 340 nm. The original traces were converted to their derivative over time ( $dA_{340}/dt$ ) to show more clearly the changes in the activities (Fig. 1B) where the decrease in  $dA_{340}/dt$  is representative of activation of ATPase and the increase is representative of inactivation. At high concentrations of ATP-Mg (above 300  $\mu M$ ), a significant activation phase (Fig. 1A and B, trace a) was observed. This is similar to the activation reported by Laget and Smith [13] and is likely to be caused by the dissociation of the  $\epsilon$  subunit from the enzyme. The rate of activation was estimated by fitting an exponential curve to the derivatised data. The rate of activation depended on the enzyme concentration, which is consistent with the hypothesis of dissociation of the  $\epsilon$  subunit from  $EF_1$ , but it did not depend on the ATP concentration when ATP concentration was above 300  $\mu M$ . (Under 300  $\mu M$  of ATP, we could not estimate the rate of activation because of the overlapping of the preceding inactivation phase (data not shown).) At intermediate concentrations of ATP (between 50  $\mu M$  and 300  $\mu M$ ), the time-courses consisted of three kinetic phases; an initial inactivation phase (increase in  $dA_{340}/dt$ ), a slow activation phase (decrease in  $dA_{340}/dt$ ), and a final, steady state (constant negative value of  $dA_{340}/dt$ )

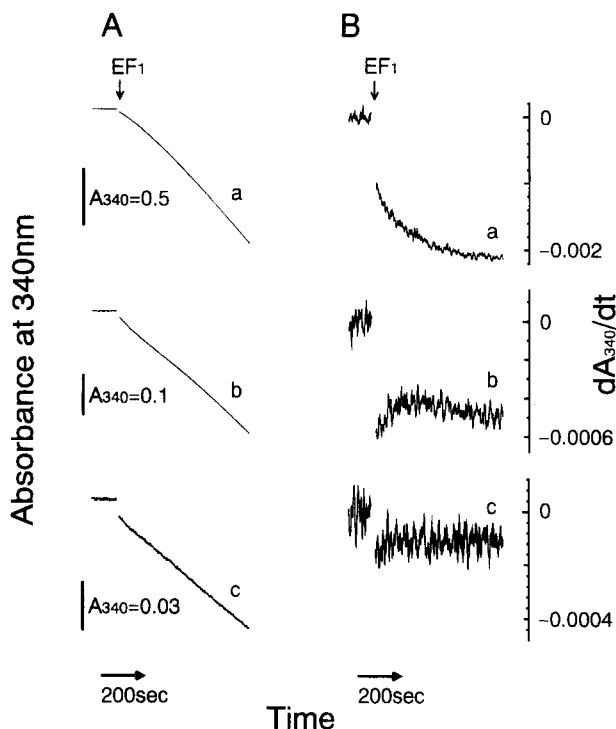


Fig. 1. Time-courses of ATP hydrolysis by nd- $\text{EF}_1$  with  $\text{F}_1$ -started reaction. The changes in absorbance at 340 nm are shown in (A) (left column). ATP concentrations were 3.7 mM (trace a), 57  $\mu\text{M}$  (trace b) and 4.4  $\mu\text{M}$  (trace c). In this case, reaction was initiated by the addition of  $\text{EF}_1$  at the time indicated by the arrow ( $\text{F}_1$ -started). The derivatives of  $A$  over time ( $dA_{340}/dt$ ) are drawn in (B) (right column).

(Fig. 1A and B, trace b). The activation phase disappeared (Fig. 1A and B, trace c) at low concentrations of ATP (between 5  $\mu\text{M}$  and 50  $\mu\text{M}$ ), and below this concentration range, there was no apparent time dependency. Results for native  $\text{EF}_1$  and nd- $\text{EF}_1$  were identical (data not shown), and therefore further experiments were carried out with nd- $\text{EF}_1$ .

### 3.2. ATP hydrolysis initiated by the addition of ATP

As stated above, the activation phase corresponds probably to the dissociation of the  $\epsilon$  subunit from the enzyme [13], however, the initial inactivation observed at relatively low ATP concentrations has not been reported for  $\text{EF}_1$  before. In order to characterize these time-dependent changes, it would be desirable to separate the inactivation phase from the activation one. Because the activation is induced by the dissociation of the  $\epsilon$  subunit and the  $K_d$  of the  $\epsilon$  and  $\text{EF}_1$  is in the order of nM [13],  $\text{EF}_1$  is spontaneously activated even in the absence of ATP when it is diluted to the nM range. In a preliminary experiment, we found that the activation of  $\text{EF}_1$  by the dilution took about 1 h at 25°C but less than 15 min at 37°C in the absence of ATP (data not shown). Thus, we first incubated the enzyme in the assay medium at a concentration of about 3 nM at 37°C for 15 min to let the  $\epsilon$  subunit dissociate from

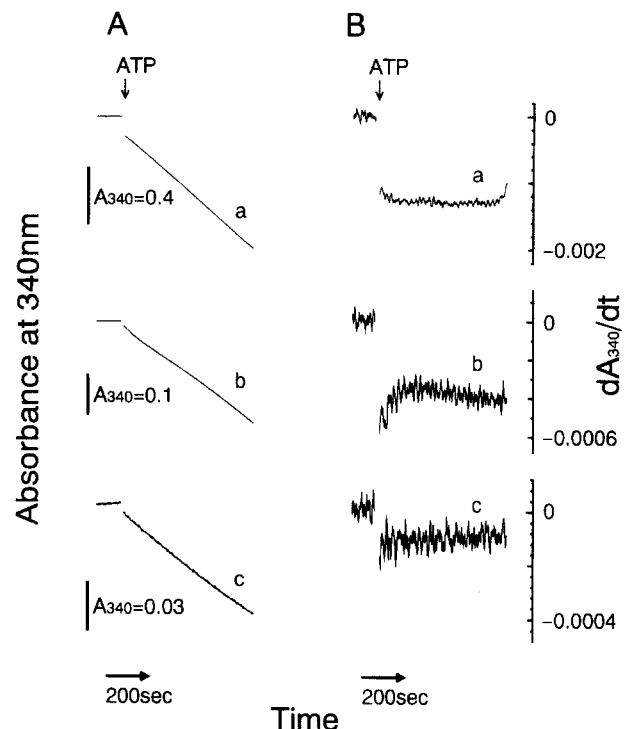


Fig. 2. Time-courses of ATP hydrolysis by nd- $\text{EF}_1$  with ATP-started reaction. In this case, reaction was initiated by the addition of ATP at the time indicated (ATP-started). ATP concentrations were 1.5 mM (trace a), 75  $\mu\text{M}$  (trace b) and 7.5  $\mu\text{M}$  (trace c). (A) and (B) are the same form as Fig. 1.

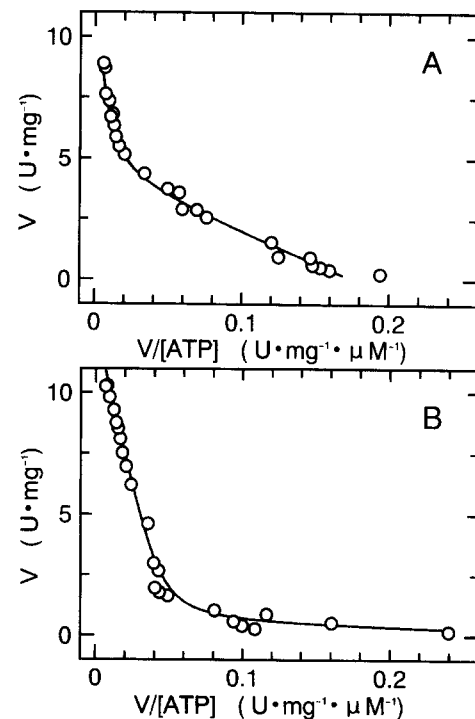
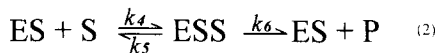
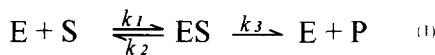


Fig. 3. Typical Eadie-Hofstee plots of ATP hydrolytic activity of nd- $\text{EF}_1$ . Data represented here are obtained from the ATP-started reaction. Solid lines are theoretical curves from determined kinetic parameters (see Fig. 5). Velocity data of (A) and (B) were obtained from the velocities at 30 s and 430 s after the initiation of the reaction, respectively.

EF<sub>1</sub>. The assay medium was then cooled down to 25°C, and the reaction was initiated by the addition of stock ATP-Mg solution (ATP-started). Typical results of ATP-started reaction are shown in Fig. 2. (A represents the original data, and B is the derivative). The activation phase at high ATP concentration observed in the F<sub>1</sub>-started reaction almost disappeared in the ATP-started reaction (compare trace a of Fig. 1A, B and Fig. 2A, B). However, there was still slight activation in the middle range of ATP concentration (Fig. 2A, B trace b). In contrast, the initial inactivation phase remained the same as that of the F<sub>1</sub>-started reaction (traces b, c). We tried to judge whether or not the rate of inactivation depends on ATP concentration. However, due to the following slight activation and the insufficient quality of the data, we could not find any clear tendency.

### 3.3. Time-dependent change in the kinetic parameters

The observation described above clearly showed that the inactivation and the activation shown at high ATP concentration were independent. Because the initial inactivation and activation phases occurred with different dependencies for ATP concentration at different time-scales, these changes were expected to affect the cooperative kinetics of ATP hydrolysis. In order to examine the time-dependent change in the kinetic parameters of ATP hydrolysis, the rate of ATP hydrolysis was calculated by least-square linear fitting on the time-course at every 50 s. From these velocity data obtained at various ATP concentrations, Eadie-Hofstee plots were constructed at various times from the start of reaction. Typical plots are shown in Fig. 3. It is clear that the shape of the Eadie-Hofstee plots change with time. In order to analyze these data, we assumed a kinetic model as shown in Scheme 1. In the ATP concentration range examined in this study, the high affinity single catalytic site is always saturated [22–24] and only the participation of the second and third catalytic sites is taken into account. (See Appendix A for details.) The kinetic parameters were determined by non-linear regression methods. The reliabilities of the parameters were checked



Scheme 1. Reaction scheme which represents negative cooperativity of ATP hydrolysis by EF<sub>1</sub>. E, S, P, ES and ESS represent the free EF<sub>1</sub>, ATP, ADP plus P<sub>i</sub>, EF<sub>1</sub>-ATP complex and EF<sub>1</sub>-2ATP complex, respectively. In this scheme, the reaction mainly proceeds as (1) in low ATP concentration and mainly as (2) in high ATP concentration. In the middle range of ATP concentration, the reaction proceeds via both (1) and (2). When  $K_m$  and  $V_{max}$  are defined as below, velocity  $\nu$  can be written as follows.  $K_{m1} = (k_2 + k_3)/k_1$ ,  $V_{max1} = k_3 \cdot [E]_0$ ,  $K_{m2} = (k_5 + k_6)/k_4$ ,  $V_{max2} = k_6 \cdot [E]_0$ ,  $\nu = ([S]^2 V_{max2} + [S] V_{max1} \cdot K_{m2}) / ([S]^2 + [S] K_{m2} + K_{m1} \cdot K_{m2})$ . See Appendix A for details.

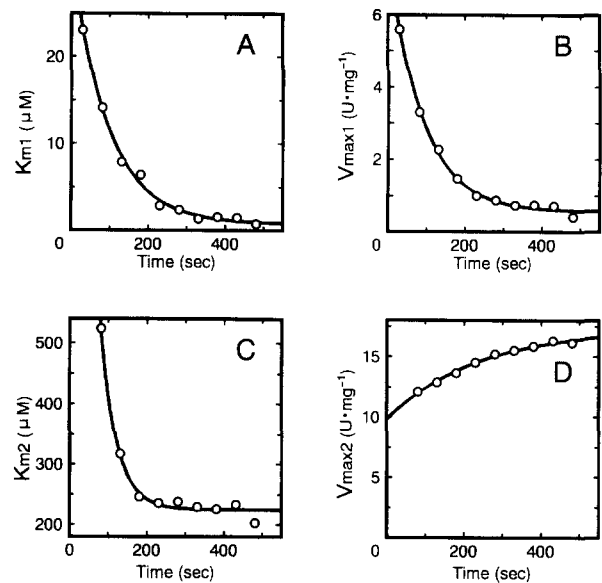


Fig. 4. Time-dependent change in the kinetic parameters for the F<sub>1</sub>-started reaction. Panels (A), (B), (C) and (D) represent time-dependent changes in  $K_{m1}$ ,  $V_{max1}$ ,  $K_{m2}$ , and  $V_{max2}$ , respectively. These values change with time as apparent first-order reactions. Solid lines are single exponential curves determined from least-square curve fitting methods. Apparent first order rate constants for the changes in  $K_{m1}$ ,  $V_{max1}$ ,  $K_{m2}$  and  $V_{max2}$  are  $1.06 \cdot 10^{-2} \text{ s}^{-1}$ ,  $1.14 \cdot 10^{-2} \text{ s}^{-1}$ ,  $2.38 \cdot 10^{-2} \text{ s}^{-1}$  and  $4.20 \cdot 10^{-3} \text{ s}^{-1}$ , respectively.

by superimposing theoretical curves on experimental data in the substrate-velocity plot and Eadie-Hofstee plot (Fig. 3, solid lines). When these parameters were plotted against time, they showed characteristic time-dependencies as

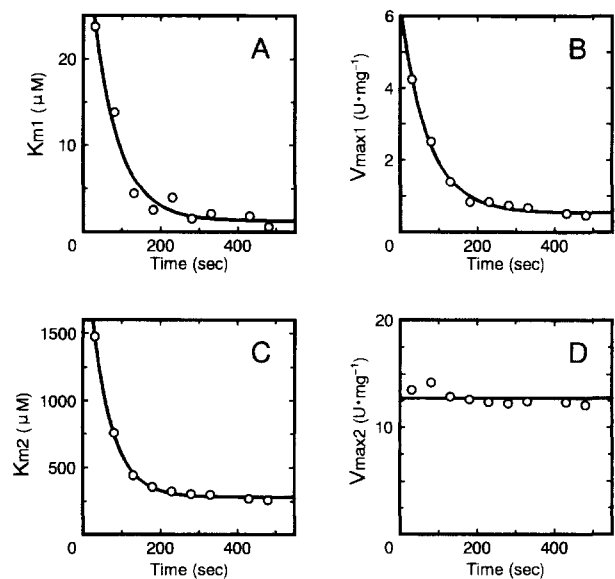


Fig. 5. Time-dependent change in the kinetic parameters with ATP-started reaction. The form of the figure is the same as Fig. 4.  $K_{m1}$ ,  $V_{max1}$ , and  $K_{m2}$  changes as apparent first-order reactions with rate constants of  $1.52 \cdot 10^{-2} \text{ s}^{-1}$ ,  $1.39 \cdot 10^{-2} \text{ s}^{-1}$ , and  $1.88 \cdot 10^{-2} \text{ s}^{-1}$ , respectively, while  $V_{max2}$  remained constant ( $12.8 \pm 0.7 \text{ U / mg}$ ).

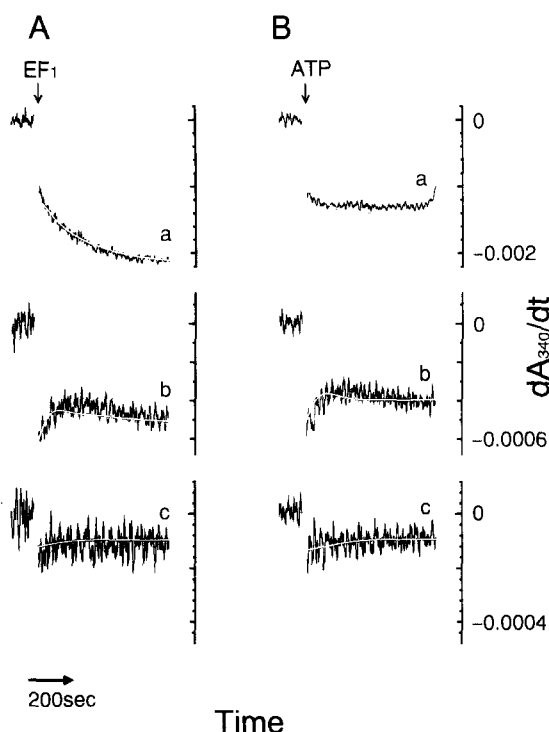


Fig. 6. Comparison of time-courses of ATPase activity of nd-EF<sub>1</sub> and theoretical lines. Time-courses of ATPase activity of nd-EF<sub>1</sub> were calculated by kinetic parameters determined with Scheme 1. (A) F<sub>1</sub>-started reaction. Traces a, b and c are same as Fig. 1B. (B) ATP-started reaction. Traces a, b and c are same as Fig. 2B. Black lines represent experimental data, and white lines represent reproduced time-courses.

shown in Fig. 4 (F<sub>1</sub>-started) and Fig. 5 (ATP-started). Except for the  $V_{\max 2}$  in the ATP-started reaction (Fig. 5D), these values changed as apparent first-order reactions, and the rate constant of the time-dependent change for each parameter was calculated by fitting with an exponential curve. The effect of the activation caused by the dissociation of the  $\epsilon$  subunit is clearly observed in the different time dependency of  $V_{\max 2}$  between F<sub>1</sub>-started and ATP-started reactions (Fig. 4D and 5D). In Fig. 4D,  $V_{\max 2}$  increases with time, reflecting the activation caused by the dissociation of the  $\epsilon$  subunit. On the other hand, when the reaction was initiated after the dissociation of the  $\epsilon$  subunit,  $V_{\max 2}$  remained essentially constant (Fig. 5D). In contrast to the activation phase, the initial inactivation is attributable to the decrease in  $V_{\max 1}$  for both types of reaction (Fig. 4B and 5B), which is about 3 times faster than the increase in  $V_{\max 2}$  (Fig. 4B and 4D). To check the validity of these analyses, the time-courses of ATPase activity were calculated from the obtained time-dependent kinetic parameters and superimposed on experimental data. They qualitatively reproduced the time-courses of the ATPase activity (Fig. 6). Thus, the complex time-dependent change in ATPase activity can be explained by a combination of independent changes in  $V_{\max}$  values associated with high and low  $K_m$  values.

#### 4. Discussion

In the present study, we have shown that the ATPase activity of EF<sub>1</sub> undergoes time-dependent inactivation and activation phases. When the ATPase reaction is initiated by the addition of enzyme (F<sub>1</sub>-started, Fig. 1), activation proceeds on a time scale of minutes. The time-dependent activation almost disappeared when the enzyme was first diluted and the ATPase reaction was initiated by the addition of ATP (ATP-started, Fig. 2). These characteristics agree well with those reported by Laget and Smith [13], and we conclude that this activation is mainly caused by the dissociation of the inhibitory  $\epsilon$  subunit from the enzyme as previously proposed [13,15]. The extent of activation observed in this study (about 1.5-fold) was not as high as that in the previous report (about 4-fold, [13]). This may be due to some dissociation of the  $\epsilon$  subunit during enzyme preparation or differences in the assay conditions. Some slight activation was still observed when the ATPase reaction was initiated by the addition of ATP (Fig. 2B, a and b). This may be caused by binding of ATP to a non-catalytic site as proposed for nd-MF<sub>1</sub> [11] or reflect incomplete dissociation of the  $\epsilon$  subunit during pre-incubation of the enzyme. In the case of EF<sub>1</sub>, however, the native enzyme containing 2 bound nucleotides and the nucleotide-depleted enzyme gave identical results. This activation was so slight that we did not further examine it precisely.

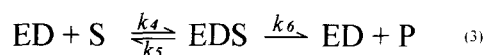
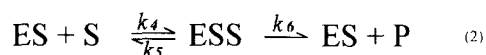
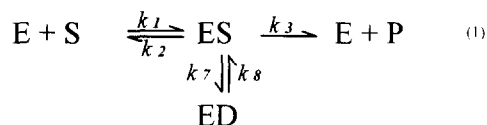
The inactivation phase of the ATPase activity of EF<sub>1</sub> was demonstrated for the first time by derivatizing the time-course data. The reason why there has been no report for the time-dependent inactivation may lie in some differences in assay conditions such as different free Mg<sup>2+</sup> concentrations, temperature or the method of determination of hydrolysis in previous studies. In fact, when the free Mg<sup>2+</sup> concentration was lower than 1 mM, or the assay was carried out at 37°C, the initial inactivation phase was not so evident (data not shown).

The most interesting finding in the present study is that the time-dependent changes in ATPase activity are closely related to the apparent cooperative kinetics of the ATPase activity of EF<sub>1</sub>. When the ATPase activity was defined at every 50 s after initiation of the reaction and Eadie-Hofstee plots were constructed, the shape of the plots changed with time (Fig. 3). Analysis of the data of the F<sub>1</sub>-started reaction according to Scheme 1 revealed that the initial inactivation phase corresponded to the decrease in  $V_{\max}$  ( $V_{\max 1}$ ) associated with low  $K_m$  ( $K_{m1}$ ) and the following activation phase corresponded to the increase in  $V_{\max}$  ( $V_{\max 2}$ ) associated with high  $K_m$  ( $K_{m2}$ ) (Fig. 4). The larger rate constant of the change in  $V_{\max 1}$  than that of  $V_{\max 2}$  reflects the fact that inactivation precedes activation. When the data for the ATP-started reaction was analyzed,  $V_{\max 1}$  decreased as in the F<sub>1</sub>-started reaction while  $V_{\max 2}$  was essentially constant (Fig. 5), which is consistent with the results that slow activation was almost absent in the

ATP-started reaction (Fig. 2). These results strongly suggest that the different kinetic modes (multiple  $K_m$  values) deduced by curve fitting actually reflect some different kinetic pathways of the ATPase reaction which can change independently.

As stated above, the increase in  $V_{\max 2}$  is mainly attributable to the dissociation of the  $\varepsilon$  subunit from the enzyme. On the other hand, the cause of the decrease in  $V_{\max 1}$  is not clear in the present study, but it may be related to the inhibition caused by ADP-Mg at a catalytic site [9]. In fact, pre-incubation of  $EF_1$  with ADP-Mg causes an inhibitory effect on the ATPase activity and the initial inactivation becomes obscure when the free  $Mg^{2+}$  concentration is lowered (data not shown). Recently Hyndman et al. [25] reported ADP-Mg inhibition of  $EF_1$  under a quite different condition (i.e., very low concentration of ATP (50 nM)). Direct comparison of the present results with those obtained under different conditions or with other  $F_1$ 's may be difficult, but it seems also related to the report that the inhibitory effect of  $NaN_3$ , which is supposed to be linked to ADP-Mg inhibition, was related to the low  $K_m$  mode of ATP hydrolysis by submitochondrial particles and isolated mitochondrial  $F_1$ -ATPase [26].

Continuous changes in the  $V_{\max}$  values may be explained as the results of the dissociation of the  $\varepsilon$  subunit ( $V_{\max 2}$ ) and ADP-Mg inhibition ( $V_{\max 1}$ ). However, it is not apparent why the  $K_m$  value changed continuously with time because conformational changes in the enzymes are generally supposed to occur between some distinct states. As for the change in  $K_{m1}$ , however, it can be explained by Scheme 2, which assumes a slow transition between the active ES complex and the inactive (or less active) ED complex. In this case, it is necessary to assume that the ED complex is still active in making the EDS complex and catalyzing the hydrolysis of ATP in the high  $K_m$  ( $K_{m2}$ ) mode because  $V_{\max 2}$  remains essentially constant in the ATP-started reaction. As for the change in  $K_{m2}$ , we could not find a good explanation. However, the slight activation



Scheme 2. Formation of inactive complex during ATP hydrolysis reaction. This scheme was derived from Scheme 1 with an additional inactivation pathway. During the ATPase reaction with the low  $K_m$  site, the inactive ED complex is formed at a very slow rate  $k_7$  and recovered at rate  $k_8$ . The ED complex is inactive in reaction (1) but still active for the high  $K_m$  mode as reaction (3) (same as reaction (2)). See Appendix B for details.

which we have ignored may affect it. Whether or not the rates of activation or inactivation depend on the ATP concentration is of interest, however, as stated in the Results section, we could not judge this point due to the insufficient quality of the data. Obviously, further rigorous analyses are required to elucidate the feature of the time-dependent change in the kinetics of  $EF_1$ .

In summary, we demonstrated the existence of the initial inactivation and successive activation phase of the ATPase activity of  $EF_1$  and found their relationship to the apparent negative cooperativity. Further precise analyses will provide insights into the mechanism of complex kinetic behavior of this enzyme.

## Acknowledgements

We thank Dr. Jean-Michel Jault for his keen interest in our work and insightful discussions and Dr. Toru Hisabori for providing us the data analysis tool, 'S.C.'.

## Appendix A

### Explanation for Scheme 1

Usually, the apparent negative cooperativity of  $F_1$ -ATPase is analyzed as a sum of two or three independent Michaelis-Menten reactions [3–5]. The kinetic parameters assuming two independent Michaelis-Menten type reactions can be converted to those from Scheme 1 in the present study as follows,

$$K_{m1} = K_{M1} \cdot K_{M2} / (K_{M1} + K_{M2})$$

$$V_{\max 1} = (V_{\max 1} \cdot K_{M2} + V_{\max 2} \cdot K_{M1}) / (K_{M1} + K_{M2})$$

$$K_{m2} = K_{M1} + K_{M2}$$

$$V_{\max 2} = V_{\max 1} + V_{\max 2}$$

Here the left columns are the parameters from Scheme 1 and the right columns (capitalized) are the parameters from two independent Michaelis-Menten type reactions. The same conclusion was derived when the data were analyzed as a sum of two Michaelis-Menten type reactions. The quality of the fit was not improved when we assumed a sum of three Michaelis-Menten reactions.

We favor Scheme 1 because it can be adopted to negative, positive and no cooperativity by choosing the appropriate set of parameters. The relationship between the range of kinetic parameters and the apparent cooperativity is summarized as follows.

Under the condition of  $V_{\max 1} < V_{\max 2}$  (substrate inhibition does not occur), and when the parameter  $C$  is defined as below, the apparent cooperativity is given by the sign of  $C$ .

$$C = V_{\max 1} \cdot K_{m2} (V_{\max 1} - V_{\max 2}) + V_{\max 2}^2 \cdot K_{m1}$$

$C > 0$ ; apparent positive cooperativity.  
 $C = 0$ ; no cooperativity.  
 $C < 0$ ; apparent negative cooperativity.

## Appendix B

### Explanation for the change in $K_{m1}$ and $V_{max1}$

The change in the kinetic parameters of the low- $K_m$  mode ( $K_{m1}$ ,  $V_{max1}$ ) may be explained by an idea that the inactivation is caused by the formation of an inactive ED complex from the ES complex as shown in Scheme 2. There are at least two possible explanations for the continuous changes in  $K_{m1}$  and  $V_{max1}$  based on this scheme.

The first possibility is that the rate of formation of the inactive complex (written as ED in Scheme 2) and the final equilibrium between ES and ED depends on the substrate concentration ( $k_7$  in Scheme 2 contains  $[S]$  as  $k_7 = k'_7 [S]$ ). In this case, at higher substrate concentration, formation of the inactive complex is faster and occurs to a greater extent. This will result in higher suppression of ATPase activity at higher substrate concentration, and the substrate concentration which gives half-maximum activity will continuously decrease as inactivation proceeds with time. In this case, the rate of inactivation will depend on the ATP concentration.

The second possibility assumes a very slow equilibrium between ES and ED, which is independent of substrate concentration ( $k_7$  in Scheme 2 does not contain  $[S]$ ). During the reaction process, ES becomes ED at a very slow rate,  $k_7$ . The ratio of ES to ES + ED ( $ES/(ES + ED)$ ) increases with time. Apparent  $K_{m1}$  and  $V_{max1}$  derived from Scheme 2 appear as  $(ES/(ES + ED)) K_{m1,0}$  and  $(ES/(ES + ED)) V_{max1,0}$ , respectively ( $K_{m1,0}$  and  $V_{max1,0}$  are values without the formation of ED ( $ES/(ES + ED) = 1$ )). In this case, the rate of inactivation will not depend on the ATP concentration but  $K_{m1}$  and  $V_{max1}$  decrease continuously with time. The first possibility is one of the variations of the second one. Similar rates of the changes in  $V_{max1}$  and  $K_{m1}$  are consistent with these ideas.

Thus, these two possibilities can be distinguished by the ATP concentration dependency of the inactivation rate.

However, due to the following slight activation phase and insufficient quality of the raw data, we could not judge whether the rate of inactivation depends on ATP concentration or not.

## References

- [1] Futai, M., Nouni, T. and Maeda, M. (1989) *Annu. Rev. Biochem.* 72, 111–136.
- [2] Boyer, P.D. (1993) *Biochim. Biophys. Acta* 1140, 215–250.
- [3] Gresser, M.J., Meyer, J.A. and Boyer, P.D. (1982) *J. Biol. Chem.* 257, 12030–12038.
- [4] Wong, S.-Y., Matsuno-Yagi, A. and Hatefi, Y. (1984) *Biochemistry* 23, 5004–5009.
- [5] Muneyuki, E. and Hirata, H. (1988) *FEBS Lett.* 234, 455–458.
- [6] Matsuda, C., Muneyuki, E., Endo, H., Yoshida, M. and Kagawa, Y. (1994) *Biochem. Biophys. Res. Commun.* 200, 671–678.
- [7] Vasilyeva, E.A., Minkov, I.B., Fitin, A.F. and Vinogradov, A.D. (1982) *Biochem. J.* 202, 15–23.
- [8] Drobinskaya, I.Y., Kozlov, I.A., Murataliev, M.B. and Vulfson, E.N. (1985) *FEBS Lett.* 182, 419–424.
- [9] Milgrom, Y.V. and Boyer, P.D. (1990) *Biochim. Biophys. Acta* 1020, 43–48.
- [10] Chernyak, B.V. and Cross, R.L. (1992) *Arch. Biochem. Biophys.* 295, 247–252.
- [11] Jault, J.-M. and Allison, W.S. (1993) *J. Biol. Chem.* 268, 1558–1566.
- [12] Milgrom, Y.M. and Murataliev, M.B. (1989) *Biochim. Biophys. Acta* 975, 50–58.
- [13] Laget, P.P. and Smith, J.B. (1979) *Arch. Biochem. Biophys.* 197, 83–89.
- [14] Smith, J.B. and Sternweis, P.C. (1977) *Biochemistry* 16, 306–311.
- [15] Dunn, S.D., Zadorozny, V.D., Tozer, R.G. and Orr, L.E. (1987) *Biochemistry* 26, 4488–4493.
- [16] Wise, J.G. (1990) *J. Biol. Chem.* 265, 10403–10409.
- [17] Senior, A.E., Lee, R.S.F., Al-Shawi, M.K. and Weber, J. (1992) *Arch. Biochem. Biophys.* 297, 340–344.
- [18] Bullough, D.A., Brown, E.L., Saario, J.D. and Allison, W.S. (1988) *J. Biol. Chem.* 263, 14053–14060.
- [19] Bradford, M.M. (1976) *Anal. Biochem.* 72, 248–254.
- [20] Stiggal, D.L., Galante, Y.M. and Hatefi, Y. (1979) *Methods Enzymol.* 55, 308–315.
- [21] Penefsky, H.S. (1977) *J. Biol. Chem.* 252, 2891–2899.
- [22] Muneyuki, E., Yoshida, M., Bullough, D.A. and Allison, W.S. (1991) *Biochim. Biophys. Acta* 1058, 304–311.
- [23] Duncan, T.M. and Senior, A.E. (1985) *J. Biol. Chem.* 260, 4901–4907.
- [24] Nouni, T., Tanai, M., Kanazawa, H. and Futai, M. (1986) *J. Biol. Chem.* 261, 9196–9201.
- [25] Hyndman, D.J., Milgrom, Y.M., Bramhall, E.A. and Cross, R.L. (1994) *J. Biol. Chem.* 269, 28871–28877.
- [26] Muneyuki, E., Makino, M., Kamata, H., Kagawa, Y., Yoshida, M. and Hirata, H. (1993) *Biochim. Biophys. Acta* 1144, 62–68.